Automatized search for hub-filament systems in numerical simulations data

Dana Makarova, Sanzhar Umbet and Dana Alina
Nazarbayev University

Cold Cores 2023
May 24 – May 26, 2023

Massive Star Formation

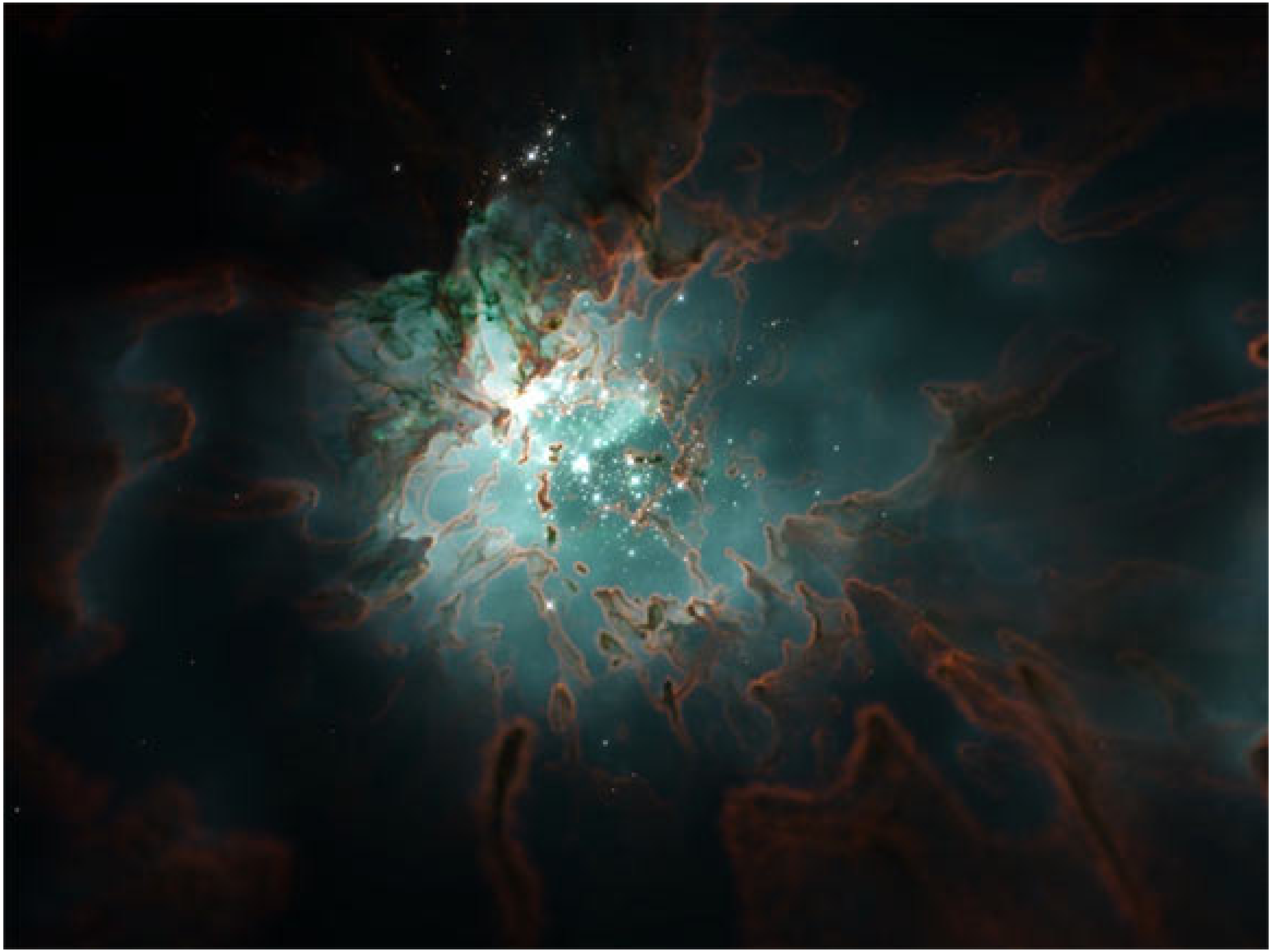

A simulated star-forming region where massive stars destroy their parent cloud.
Image credit: STARFORGE (STAR FORmation in Gaseous Environments).

One of the clearest example of HFSs
Mon R2

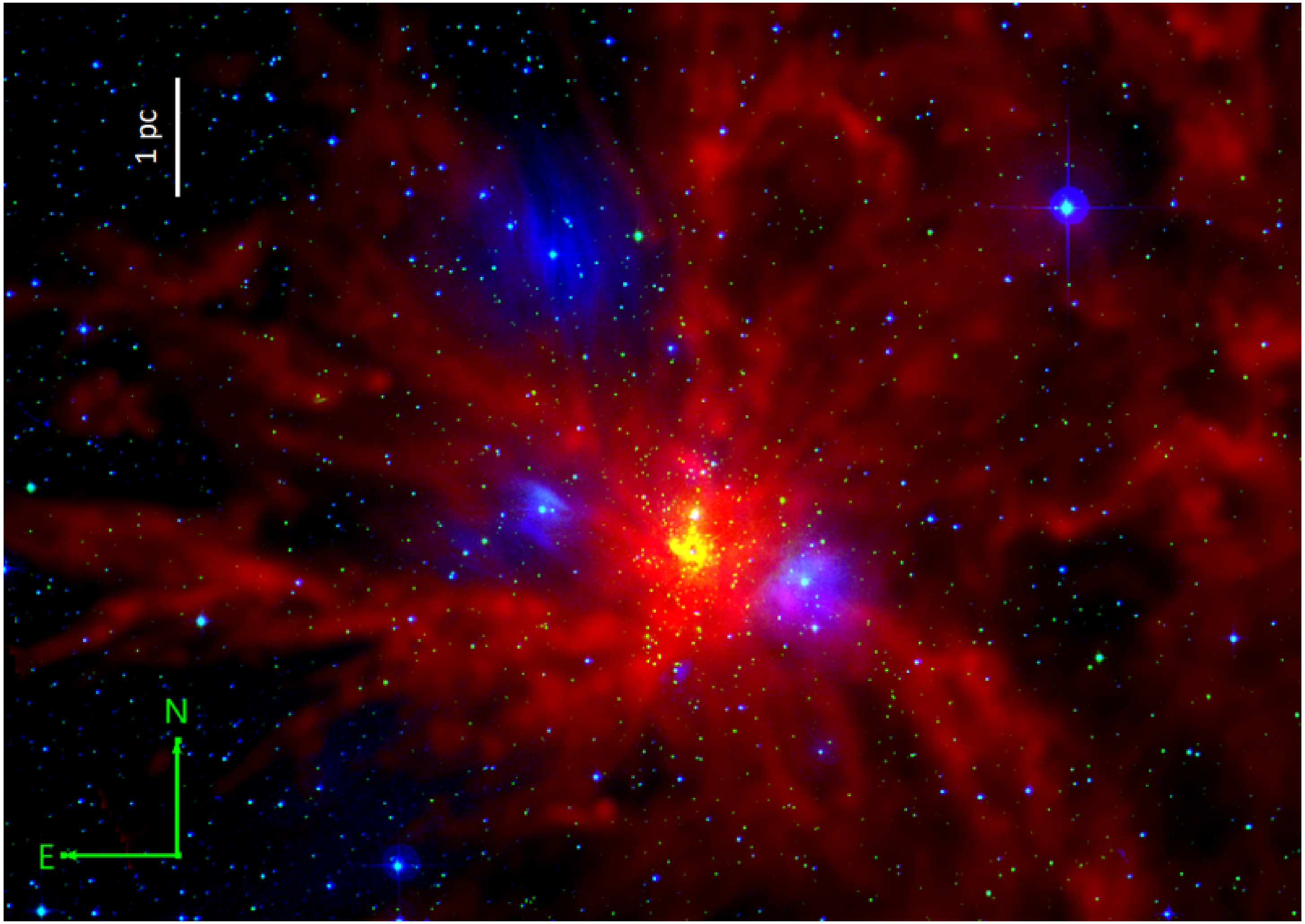

Three-color image of the Mon R2 cluster-forming hub-filaments system
Red: H2 column density map derived from Herschel SPIRE and PACS observations (Didelon et al. 2015), green: 1.65 μm band of the Two Micron All Sky Survey (Skrutskie et al. 2006), and blue: 560 nm band of the Digitalized Sky Survey (Lasker et al. 1990).

One of the clearest examples of HFSs Mon R2

- Main filaments
- Secondary filaments
- Main filaments extend into the central hub
- Ring-shaped or spiral morphology within the hub

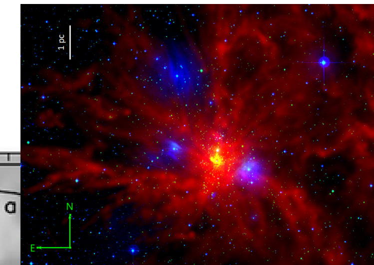

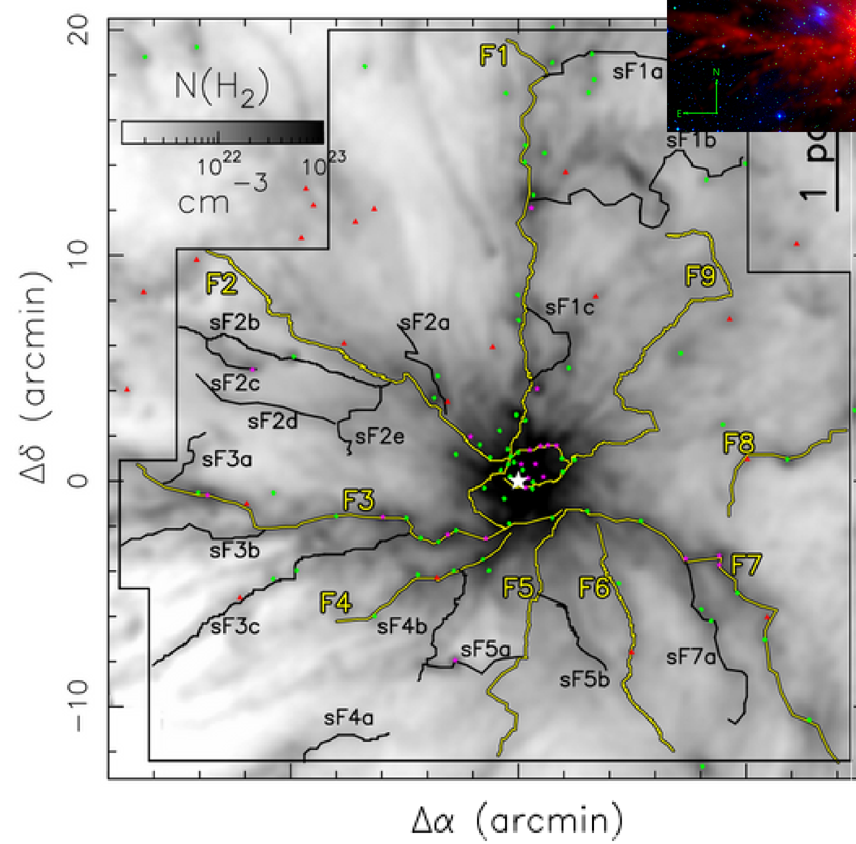

H2 column density maps from Herschel. The "skeleton" of identified filaments are marked with solid black or yellow lines. (Didelon et al. 2015).

Examples of HFSs

NGC 6334

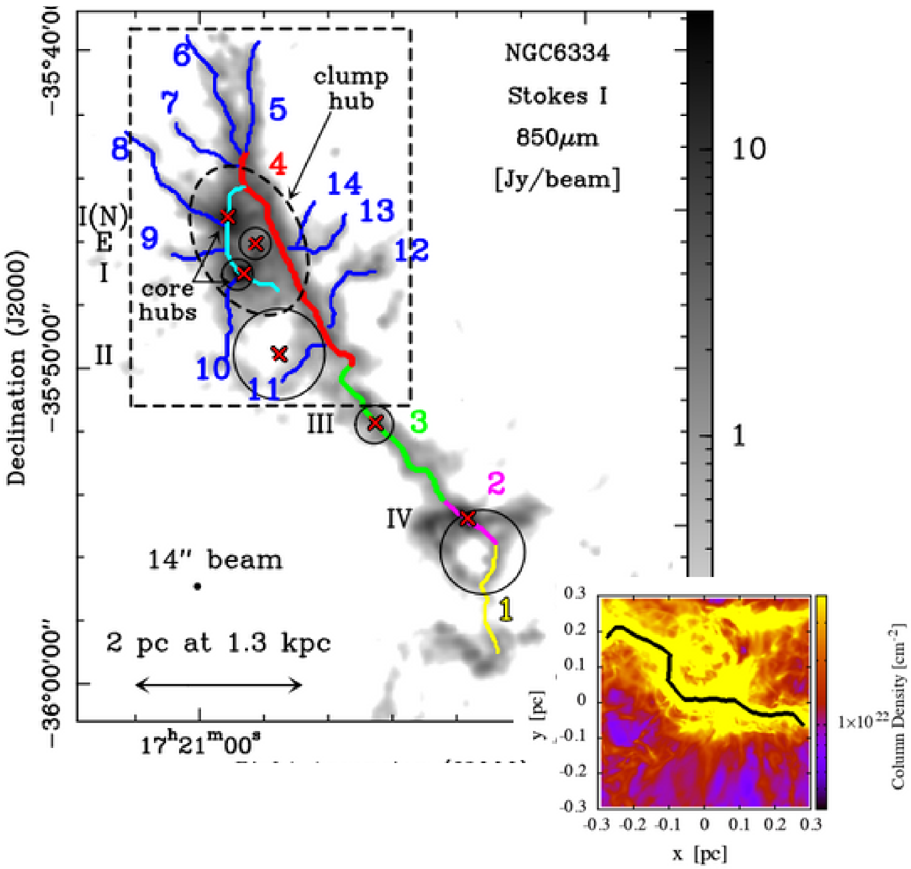

Upper: The crests of the identified filamentary structures (Arzoumanian et al. 2021); *Lower:* Column density map of the filament. The black curve shows the crest of the filament traced with FilFinder (Koch & Rosolowsky 2015).

IC5146

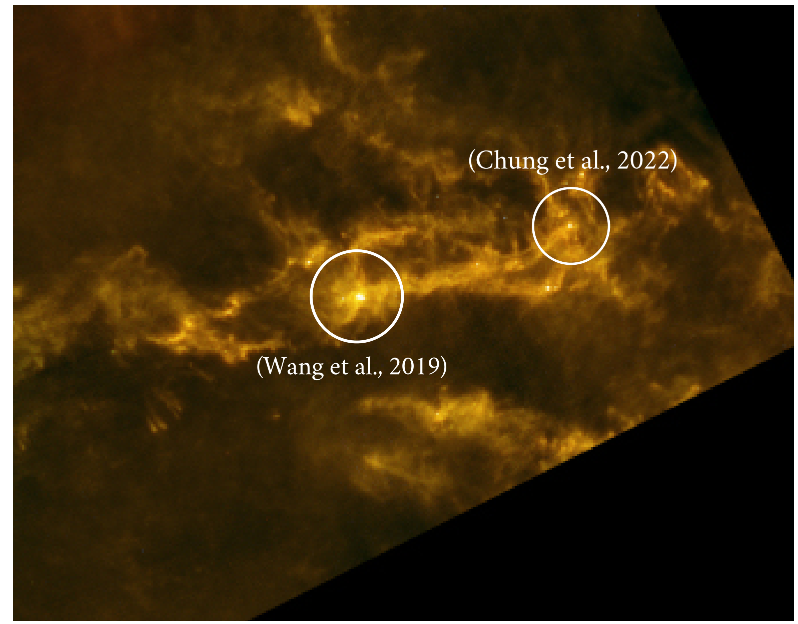

Composite 3-color image of IC 5146 (Arzoumanian et al., 2011).

Hub Filament Systems

01

are the highest density regions where several filaments converge. (Treviño-Morales et al., 2019)

02

are junctions of filaments, which are high column density and low aspect ratio objects. (Kumar et al., 2022)

03

are often host most of the star formation in a filamentary cloud and hence are the potential sites for cluster formation. (Wang et al., 2019)

04

are regions that host a number of clumps in different phases, where observed an active high-mass star formation. (Arzoumanian et al., 2021)

Simulations

SND
Supernova-driven magnetohydrodynamic simulation

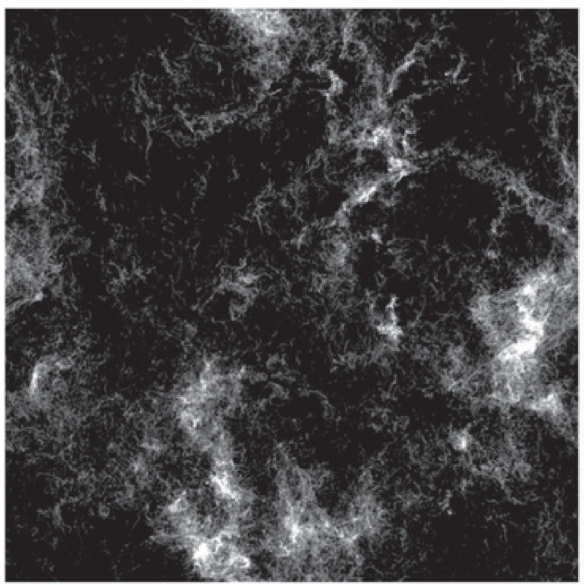

(Padoan et al., 2020, Lu et al., 2021)

3 datacubes
at 15.4, 23.3, and 34.2 Myr
after self-gravity included;

Size: 250 pc;

Self-gravity included at 55.5 Myr.

The Enzo Project - ENZO
Isothermal, self-gravitating, supersonic magnetohydrodynamic simulation

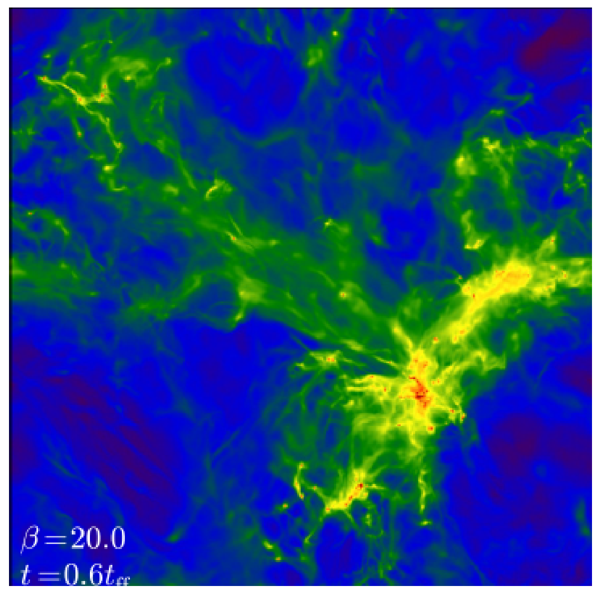

(Collins et al. 2012, Burkhart et al. 2015)

9 datacubes
at 0.1, 0.3, and 0.6 t_{ff}
for β_0 = 0.2, 2, and 20,
where the cloud-averaged freefall time is $t_{\rm ff} = (3\pi/32G\rho_0)^{1/2}$
and β_0 - mean thermal-to-magnetic pressure ratio.

The Galactica simulation database - LS
Turbulent, self-gravitating and magnetized interstellar medium simulation

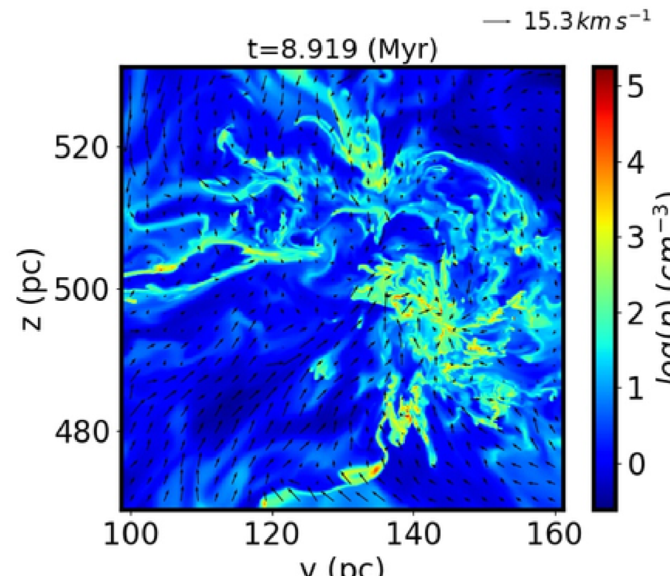

(Hennebelle & Iffrig 2014, Iffrig & Hennebelle 2017)

6 datacubes at two times
for 3, 6, and 12 μG;

Size: 1 kpc.

Algorithm

- **Preprocessing**
- **Morphological criterium**
- **Density criterium**
- **Velocity criterium**

Algorithm - Preprocessing

SCIMES
(Spectral Clustering for Molecular Emission Segmentation)
(Colombo et al., 2015)

Skeletonization

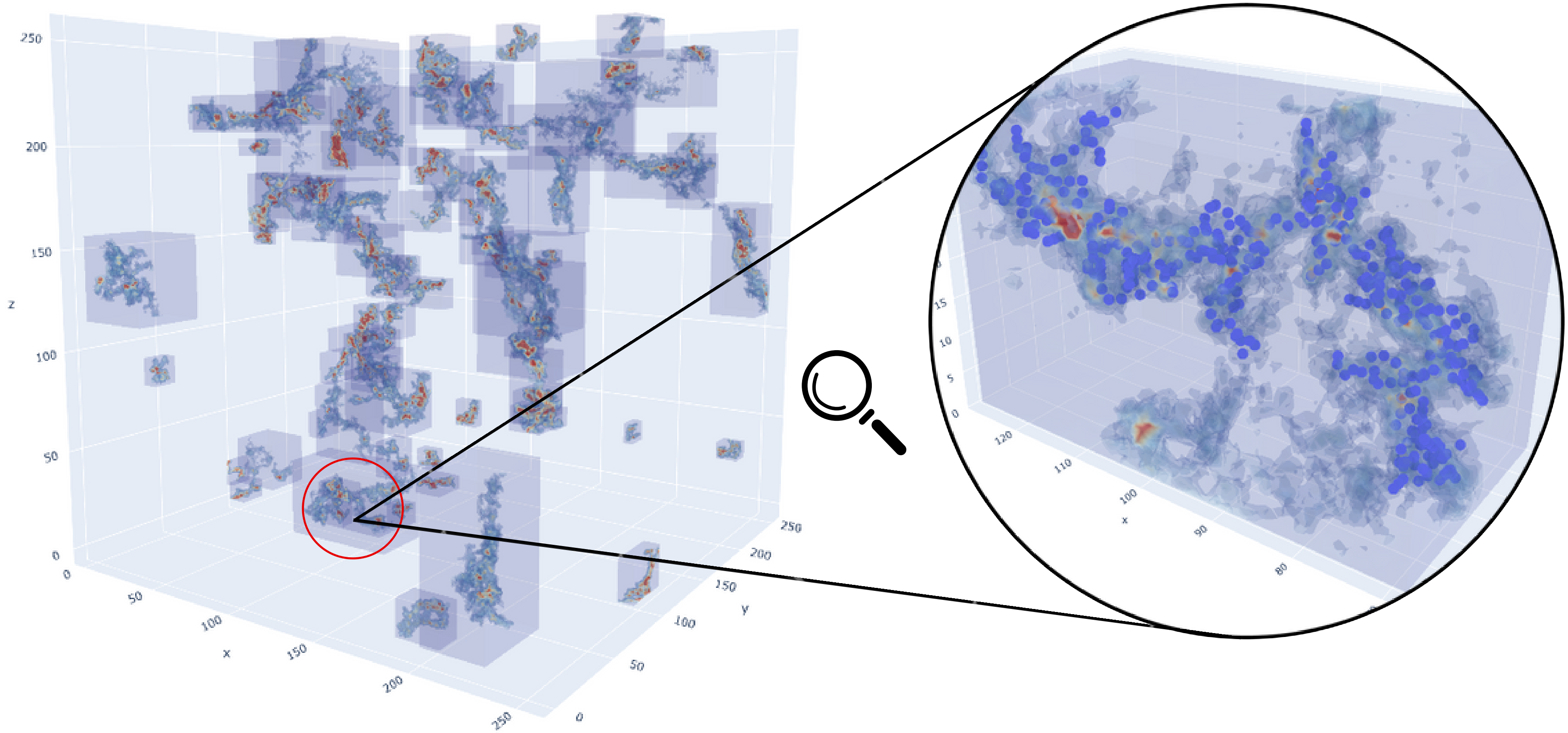

The alternative ways of the clusterization are also applicable.
Left: The example of SCIMES clustering in the data cube.
Right: The example of a SCIMES cluster and its skeleton.

Algorithm - Morphological criterium

Branches criterium relies on the branches' count of each potential node. If a node has three or more branches, then it is marked as a node.

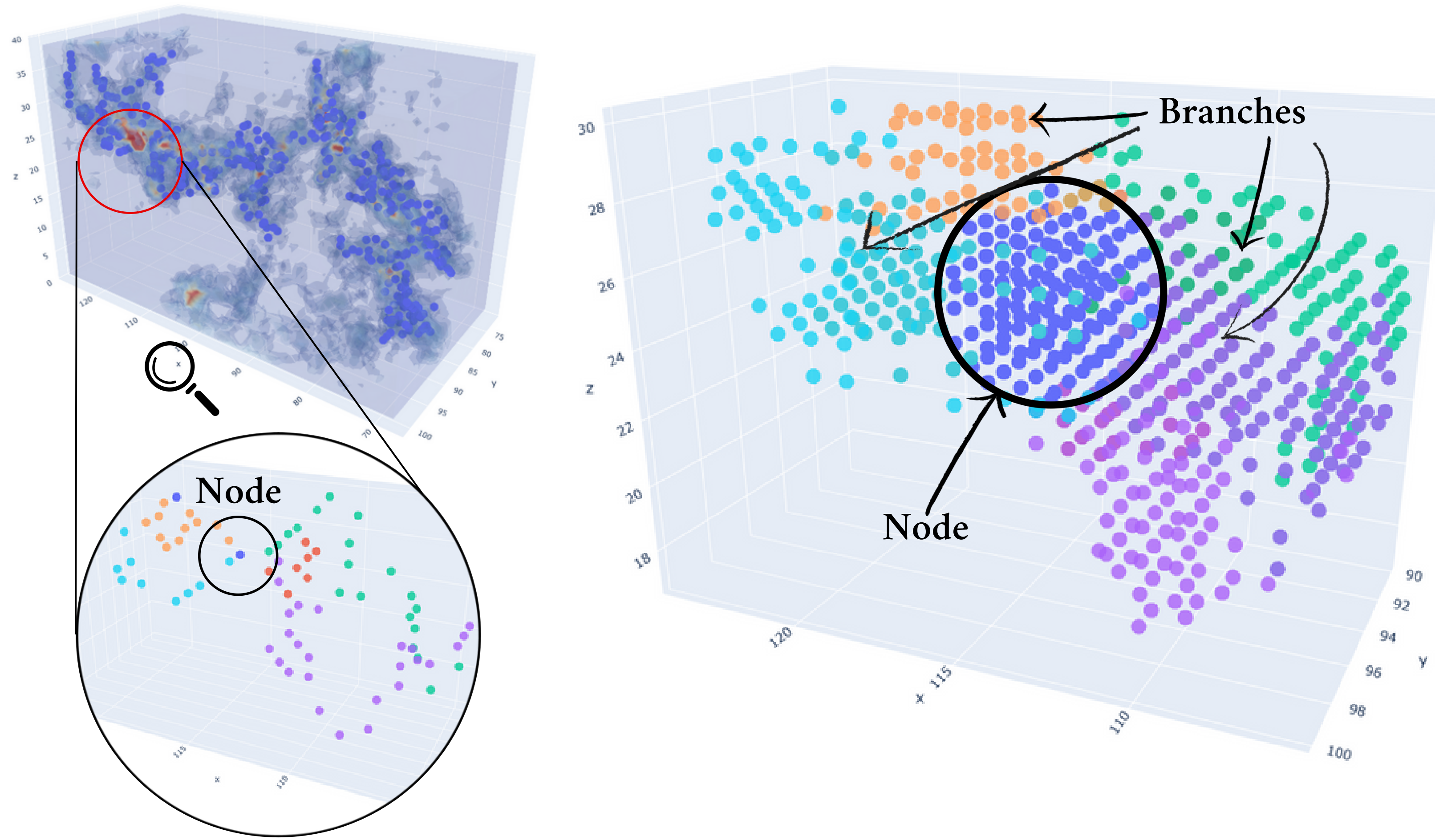

Upper left: The example of a SCIMES cluster.
Lower left: The example of the identified node and its skeletonized branches.
Right: The example of the identified node and its branches in volume.

Algorithm - Physical criterium

Density criterium checks if the node is the local density maximum.

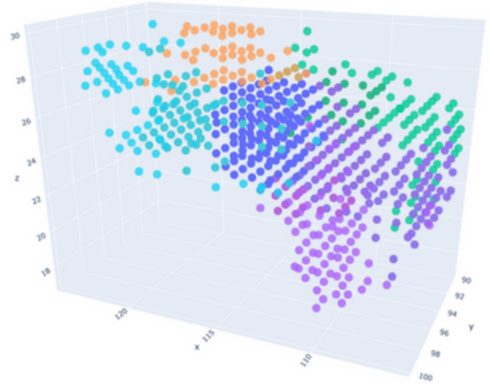

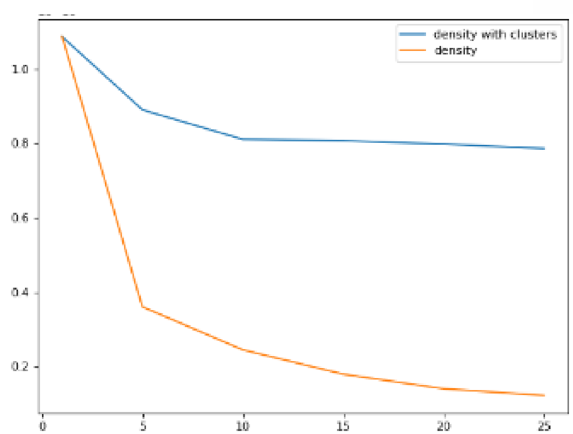

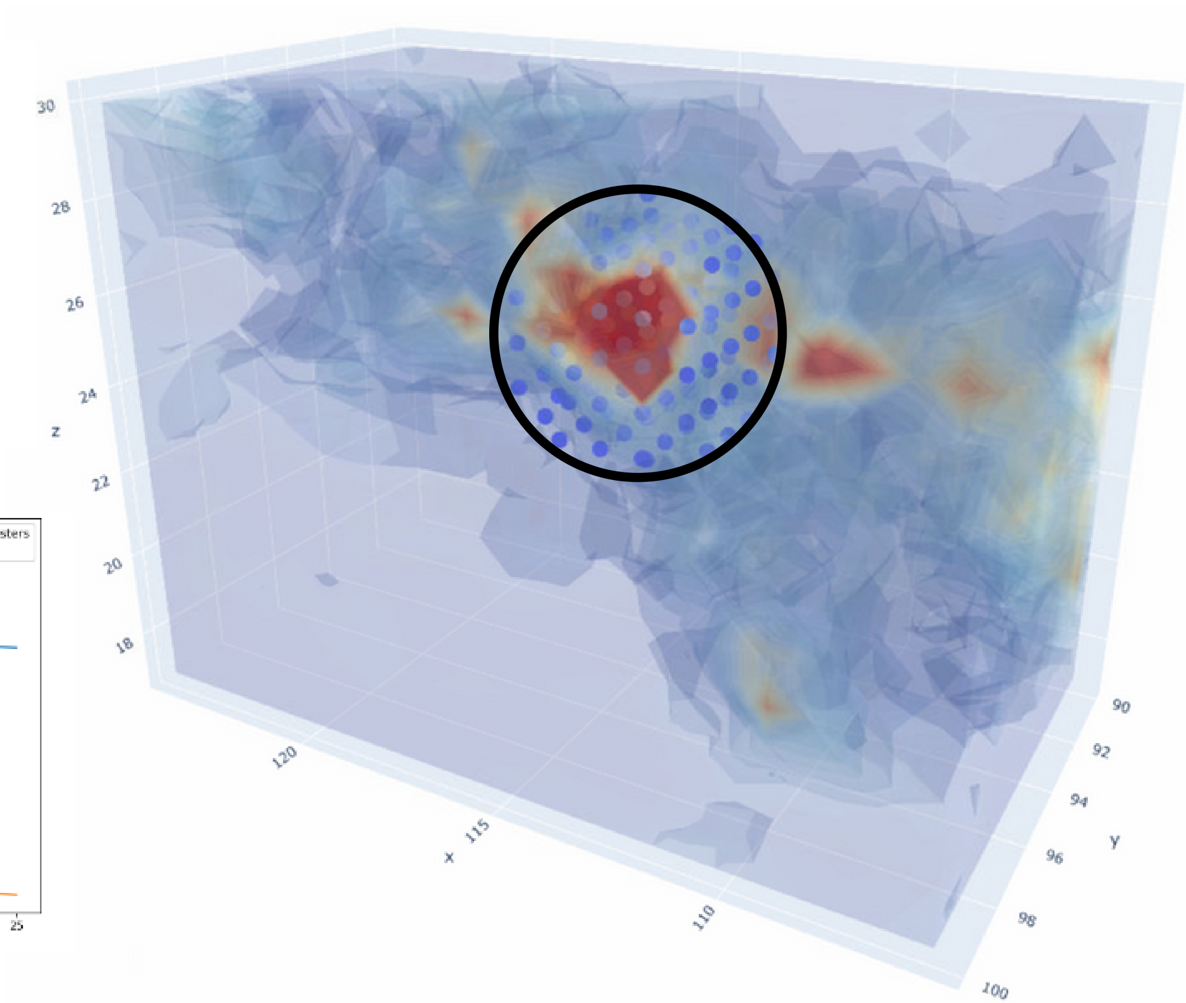

Upper left: The example of the identified node and its branches in volume.
Lower left: The radial profile of the density.
Right: The example of the identified node's density.

Algorithm - Physical criterium

Velocity criterium checks the velocity uniformity and the branches inflow.

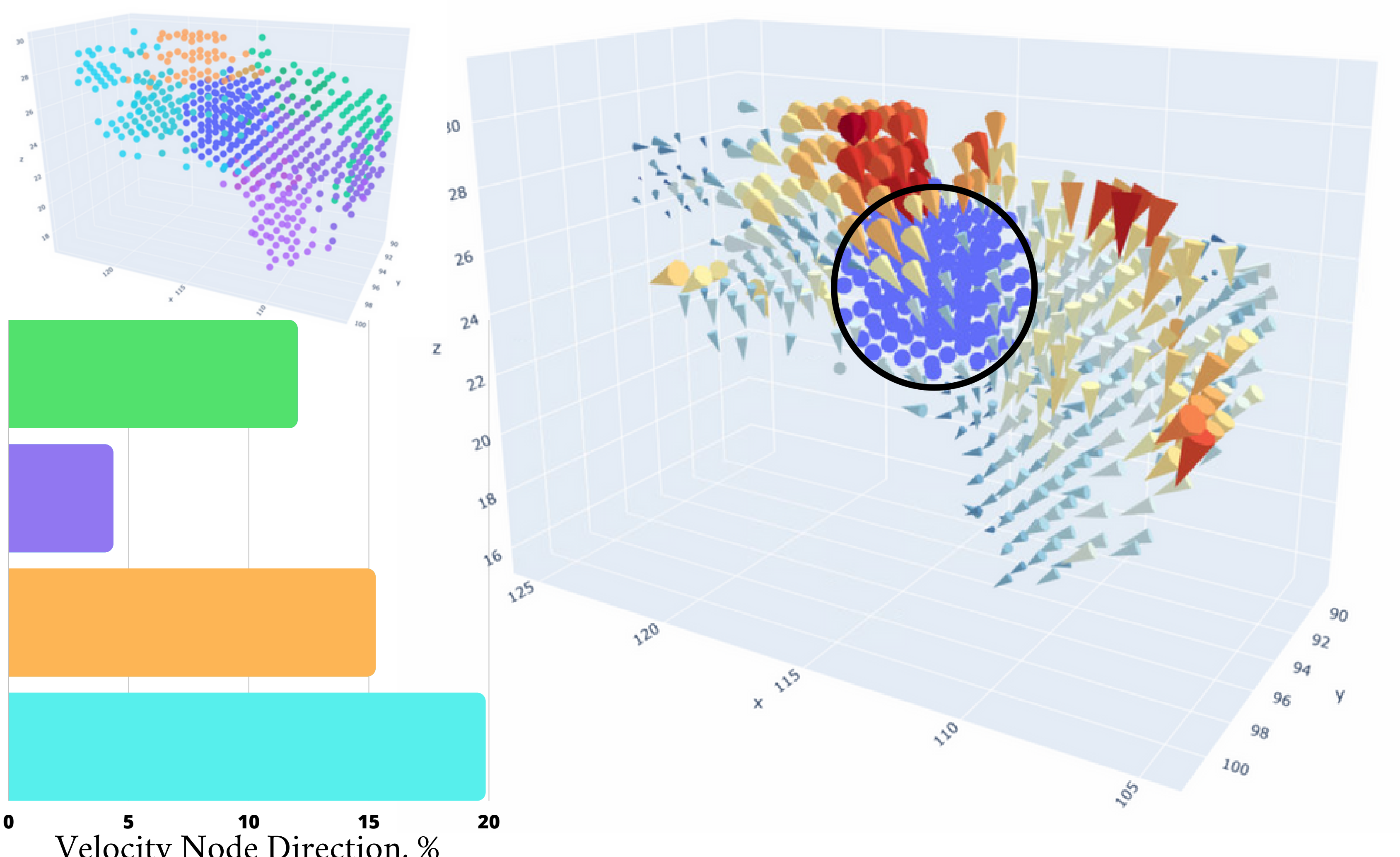

Upper left: The example of the identified node and its branches in volume.
Lower left: The branches' velocity direction histogram.
Right: The example of the identified node's velocity field.

Results - SND

Statistics of the resulted number of clusters and potential hubs

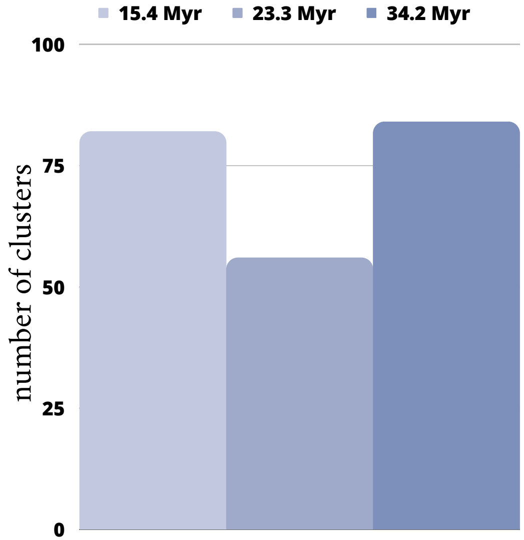

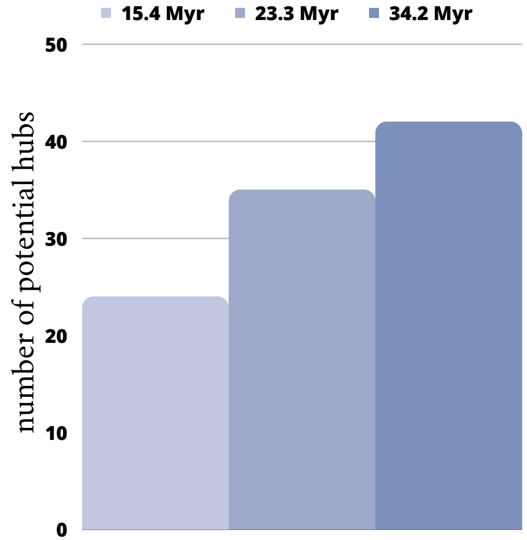

Example of the potential hub

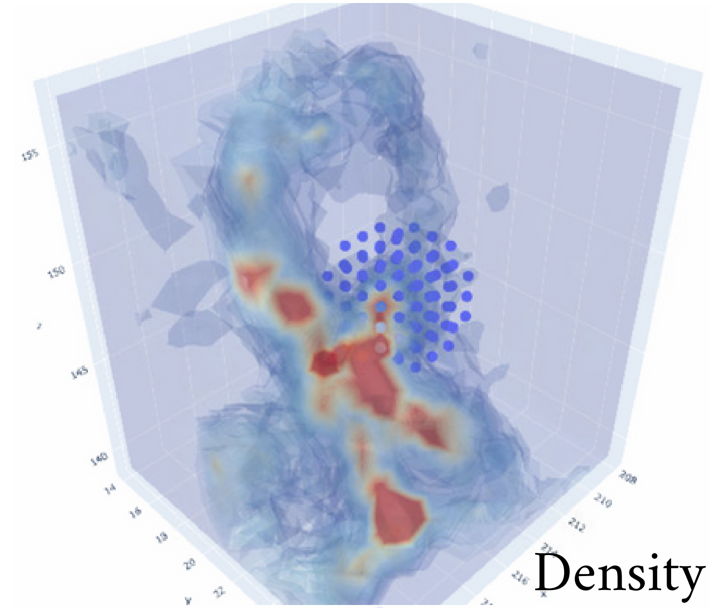

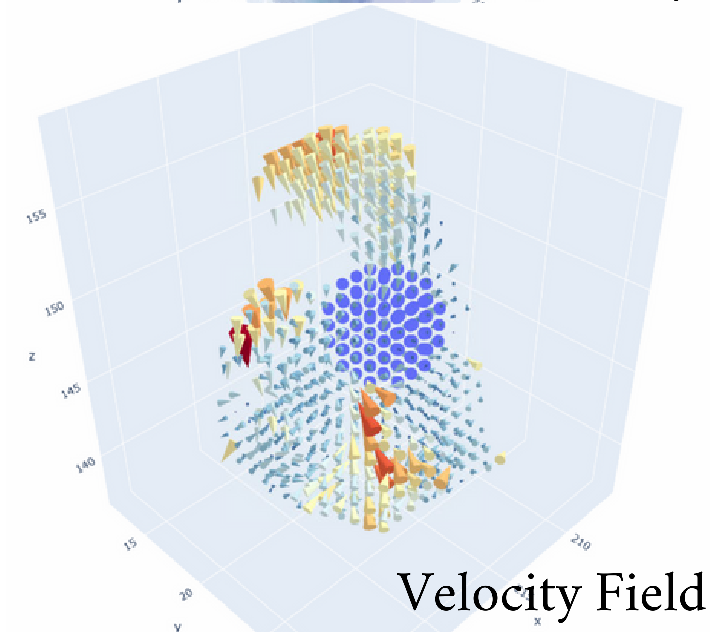

Examples of the nodes elimination

Cube*	Step 1, N	Step 2, N	Step 3, N
SND t = 23.5 Myr	1382	72	35
SND t = 34.2 Myr	1245	86	42

Results - SND

Statistics of the resulted number of clusters and potential hubs

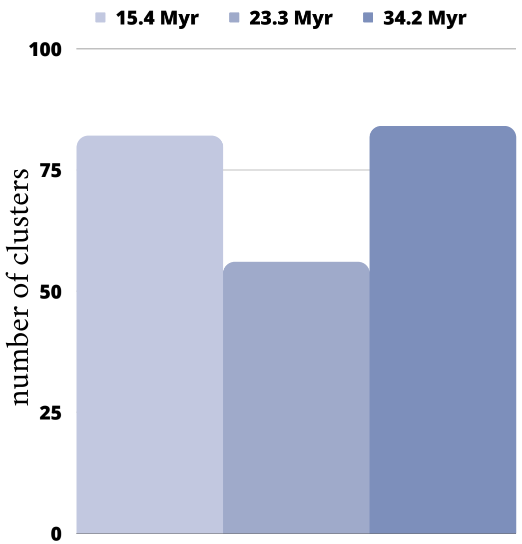

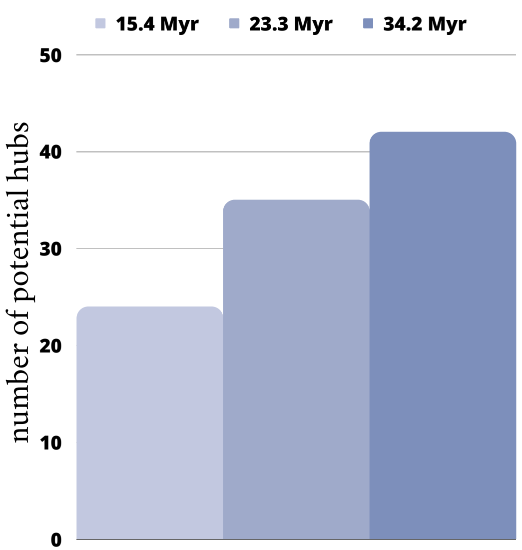

The amount of clusters is inversely proportional to the star-formation rate.

The amount of potential hubs is proportional to the star-formation efficiency.

Results - ENZO

Statistics of the resulted number of clusters and potential hubs

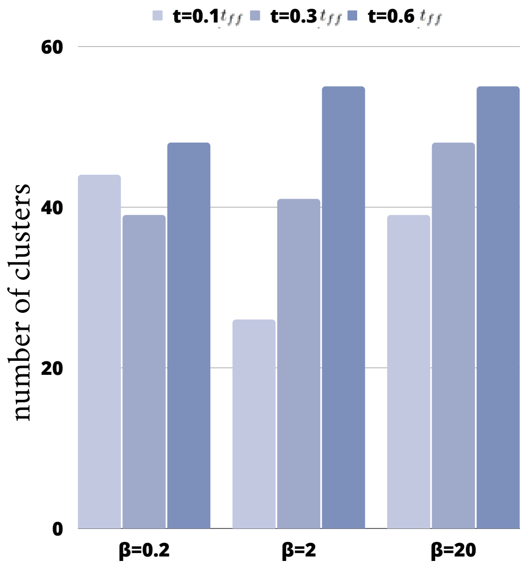

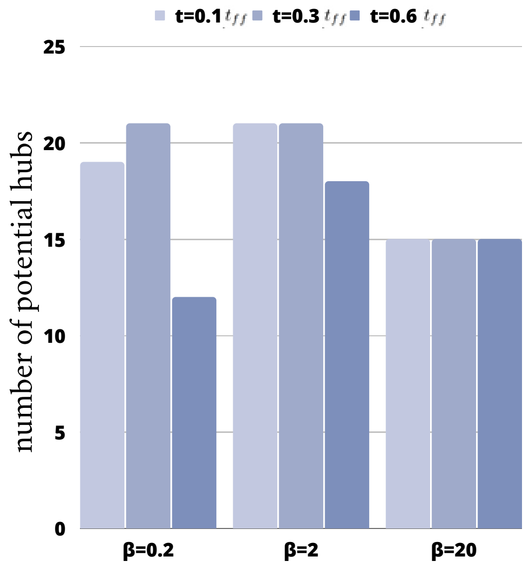

Example of the potential hub

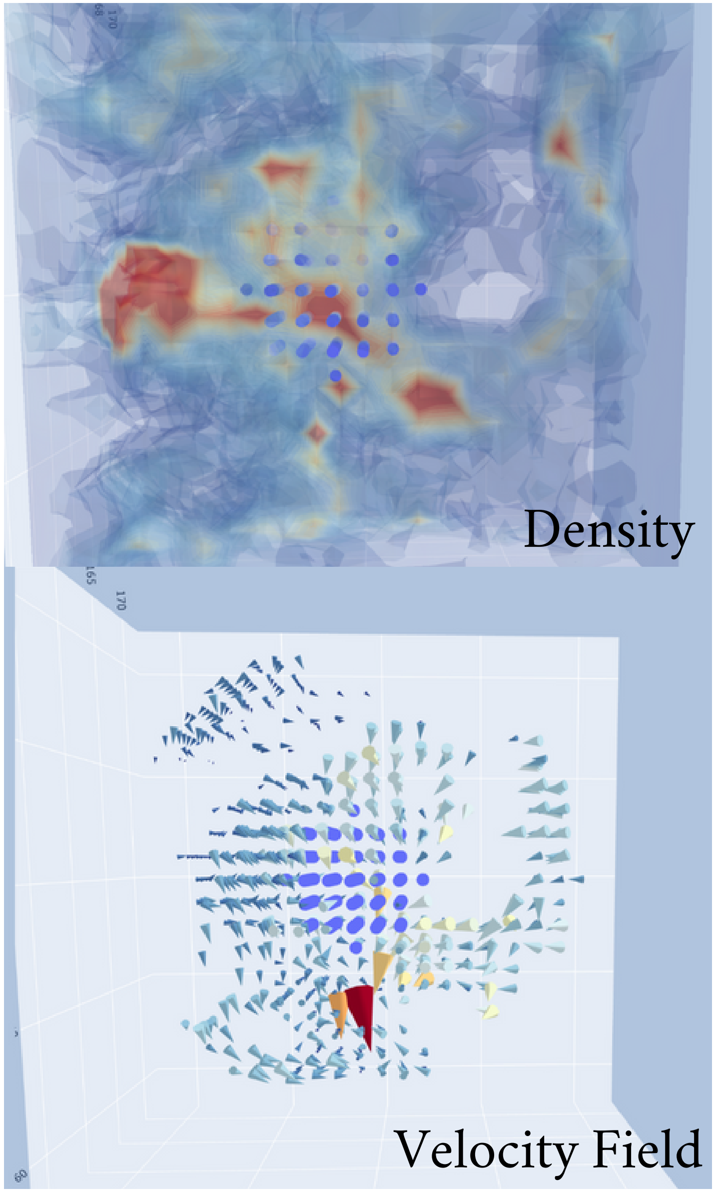

Examples of the nodes elimination

Cube*	Step 1, N	Step 2, N	Step 3, N
ENZO β=2, $t=0.1t_{ff}$	443	43	19
ENZO β=2, $t=0.3t_{ff}$	222	9	4

Results - ENZO

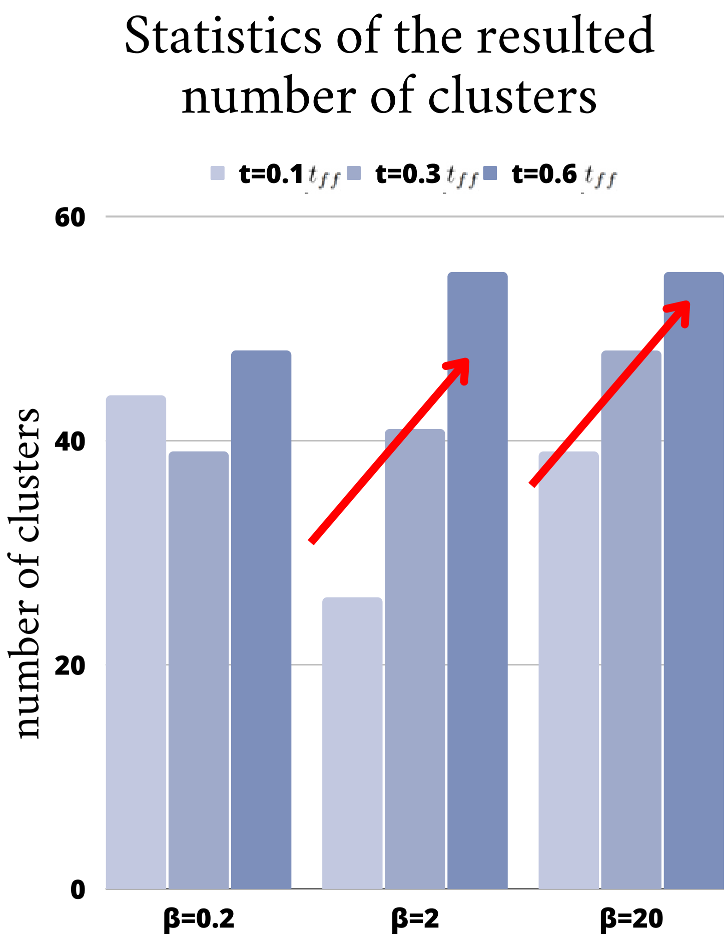

The amount of clusters increases with time for β=2 and β=20.

Results - LS

Statistics of the resulted number of clusters and potential hubs

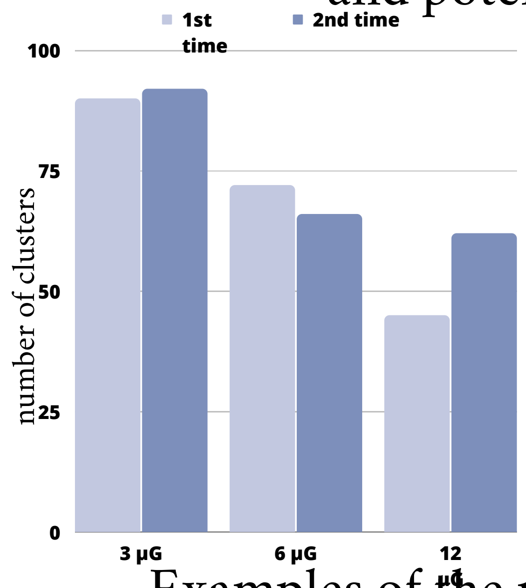

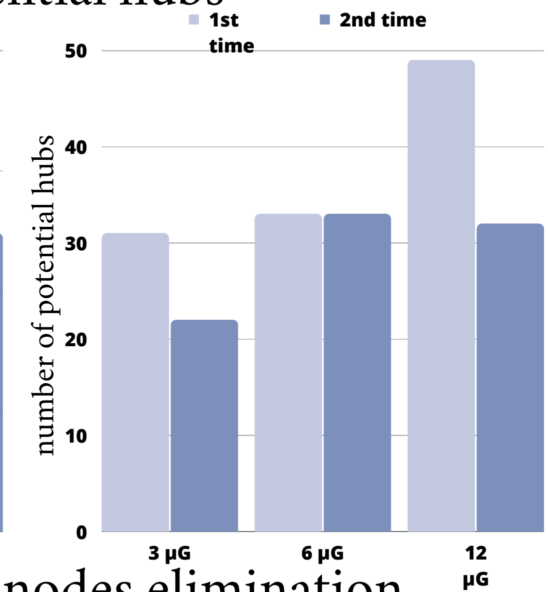

Example of the potential hub

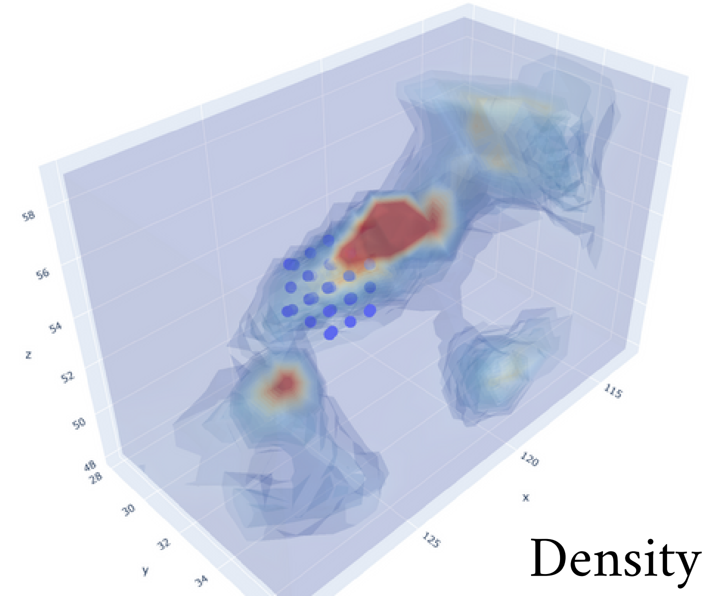

Density

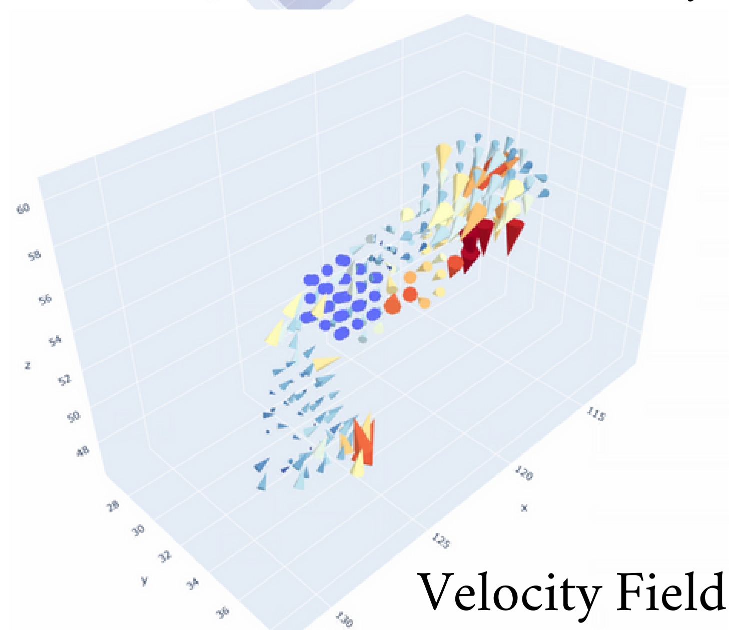

Velocity Field

Examples of the nodes elimination

Cube*	Step 1, N	Step 2, N	Step 3, N
LS B=3μG, t=50.2kyr	443	31	12
LS B=3μG, t=74.7kyr	320	22	8

Results - LS

Statistics of the resulted number of clusters

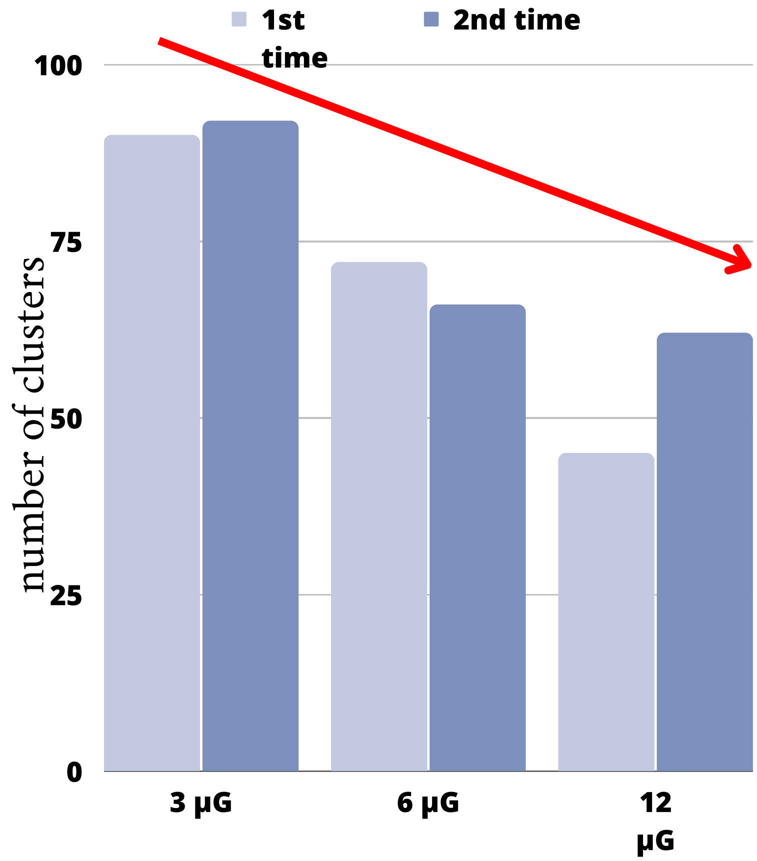

The number of clusters decreases as magnetization increases.

Summary

- Method for the identifying HFSs in the 3D-simulation data.
- Three-step method is highly efficient in removing almost 98% of falsely identified hubs.
- Different clusterization methods applicable for preprocessing (e.g. density threshold, DBSCAN, etc.)
- Potential hub-filament systems do not persist through the different epochs of one simulation.
- The amount of the potential hubs increases with the star-formation efficiency in SND.
- The amount of SCIMES clusters is increases with time in ENZO and decreases as magnetization increases in LS.

Objectives

- Derive characteristic properties of the found simulated potential hubs
- Create synthetic observations out of the found hub-filament systems
- Analyze the obtained synthetic observations
- Try to adopt the algorithm for the observational data

Reference List

- Arzoumanian, D., André, Ph., Didelon, P., Könyves, V., Schneider, N., Men'shchikov, A., Sousbie, T., Zavagno, A., Bontemps, S., Di Francesco, J., Griffin, M., Hennemann, M., Hill, T., Kirk, J., Martin, P., Minier, V., Molinari, S., Motte, F., Peretto, N., … Wilson, C. D. (2011). Characterizing interstellar filaments withherschelin IC 5146. Astronomy & Astrophysics, 529. https://doi.org/10.1051/0004-6361/201116596
- Arzoumanian, D., Furuya, R. S., Hasegawa, T., Tahani, M., Sadavoy, S., Hull, C. L., Johnstone, D., Koch, P. M., Inutsuka, S., Doi, Y., Hoang, T., Onaka, T., Iwasaki, K., Shimajiri, Y., Inoue, T., Peretto, N., André, P., Bastien, P., Berry, D., … van Loo, S. (2021). Dust polarized emission observations of NGC 6334. Astronomy & Astrophysics, 647. https://doi.org/10.1051/0004-6361/202038624
- Burkhart, B., Collins, D. C., & Lazarian, A. (2015). Observational diagnostics of self-gravitating MHD turbulence in giant molecular clouds. The Astrophysical Journal, 808(1), 48. https://doi.org/10.1088/0004-637x/808/1/48
- Chung, E. J., Lee, C. W., Kwon, W., Yoo, H., Soam, A., & Cho, J. (2022). Evolution of the hub-filament structures in IC 5146 in the context of the energy balance of gravity, turbulence, and magnetic field. The Astronomical Journal, 164(5), 175. https://doi.org/10.3847/1538-3881/ac8a43
- Collins, D. C., Kritsuk, A. G., Padoan, P., Li, H., Xu, H., Ustyugov, S. D., & Norman, M. L. (2012). The two states of Star-forming clouds. The Astrophysical Journal, 750(1), 13. https://doi.org/10.1088/0004-637x/750/1/13
- Colombo, D., Rosolowsky, E., Ginsburg, A., Duarte-Cabral, A., & Hughes, A. (2015). Graph-based interpretation of the molecular interstellar medium segmentation. Monthly Notices of the Royal Astronomical Society, 454(2), 2067–2091. https://doi.org/10.1093/mnras/stv2063
- Didelon, P., Motte, F., Tremblin, P., Hill, T., Hony, S., Hennemann, M., Hennebelle, P., Anderson, L. D., Galliano, F., Schneider, N., Rayner, T., Rygl, K., Louvet, F., Zavagno, A., Könyves, V., Sauvage, M., André, Ph., Bontemps, S., Peretto, N., … White, G. J. (2015). From forced collapse to H II region expansion in mon R2: Envelope density structure and age determination withherschel. Astronomy & Astrophysics, 584. https://doi.org/10.1051/0004-6361/201526239
- Hennebelle, P., & Iffrig, O. (2014). Simulations of magnetized multiphase galactic disc regulated by Supernovae Explosions. Astronomy & Astrophysics, 570. https://doi.org/10.1051/0004-6361/201423392
- Iffrig, O., & Hennebelle, P. (2017). Structure distribution and turbulence in self-consistently supernova-driven ISM of multiphase magnetized galactic discs. Astronomy & Astrophysics, 604. https://doi.org/10.1051/0004-6361/201630290
- Koch, E. W., & Rosolowsky, E. W. (2015). Filament identification through mathematical morphology. Monthly Notices of the Royal Astronomical Society, 452(4), 3435–3450. https://doi.org/10.1093/mnras/stv1521
- Kumar, M. S., Arzoumanian, D., Men'shchikov, A., Palmeirim, P., Matsumura, M., & Inutsuka, S. (2022). Filament coalescence and hub structure in mon R2. Astronomy & Astrophysics, 658. https://doi.org/10.1051/0004-6361/202140363
- Lasker, B. M., Sturch, C. R., McLean, B. J., Russell, J. L., Jenkner, H., & Shara, M. M. (1990). The Guide Star Catalog. I - astronomical foundations and image processing. The Astronomical Journal, 99, 2019. https://doi.org/10.1086/115483
- Lu, Z.-J., Pelkonen, V.-M., Juvela, M., Padoan, P., Haugbølle, T., & Nordlund, Å. (2021). Physical properties and real nature of massive clumps in the galaxy. Monthly Notices of the Royal Astronomical Society, 510(2), 1697–1715. https://doi.org/10.1093/mnras/stab3517
- Padoan, P., Pan, L., Juvela, M., Haugbølle, T., & Nordlund, Åke. (2020). The origin of massive stars: The inertial-inflow model. The Astrophysical Journal, 900(1), 82. https://doi.org/10.3847/1538-4357/abaa47
- Skrutskie, M. F., Cutri, R. M., Stiening, R., Weinberg, M. D., Schneider, S., Carpenter, J. M., Beichman, C., Capps, R., Chester, T., Elias, J., Huchra, J., Liebert, J., Lonsdale, C., Monet, D. G., Price, S., Seitzer, P., Jarrett, T., Kirkpatrick, J. D., Gizis, J. E., … Wheelock, S. (2006). The Two micron all sky survey (2MASS). The Astronomical Journal, 131(2), 1163–1183. https://doi.org/10.1086/498708
- Starforge. (2022, August 5). https://starforge.space/index.html
- Treviño-Morales, S. P., Fuente, A., Sánchez-Monge, Á., Kainulainen, J., Didelon, P., Suri, S., Schneider, N., Ballesteros-Paredes, J., Lee, Y.-N., Hennebelle, P., Pilleri, P., González-García, M., Kramer, C., García-Burillo, S., Luna, A., Goicoechea, J. R., Tremblin, P., & Geen, S. (2019). Dynamics of cluster-forming hub-filament systems. Astronomy & Astrophysics, 629. https://doi.org/10.1051/0004-6361/201935260
- Wang, J.-W., Lai, S.-P., Eswaraiah, C., Pattle, K., Francesco, J. D., Johnstone, D., Koch, P. M., Liu, T., Tamura, M., Furuya, R. S., Onaka, T., Ward-Thompson, D., Soam, A., Kim, K.-T., Lee, C. W., Lee, C.-F., Mairs, S., Arzoumanian, D., Kim, G., … Zhu, L. (2019). JCMT bistro survey: Magnetic Fields within the hub-filament structure in IC 5146. The Astrophysical Journal, 876(1), 42. https://doi.org/10.3847/1538-4357/ab13a2
- This work reused datasets available on the:
  - https://www.erda.dk/vgrid/massive-clumps/
  - https://www.mhdturbulence.com/
  - Galactica simulations database (http://www.galactica-simulations.eu)